Electronic Supplementary Information for

Healable and Shape Editable Supercapacitors Based on Shape Memory Polyurethanes

Tianqi Li, Xu Fang, Qiang Pang, Weimin Huang, and Junqi Sun*

State Key Laboratory of Supramolecular Structure and Materials, College of Chemistry, Jilin University, Changchun 130012, People's Republic of China

*Corresponding authors. E-mail: sun_junqi@jlu.edu.cn

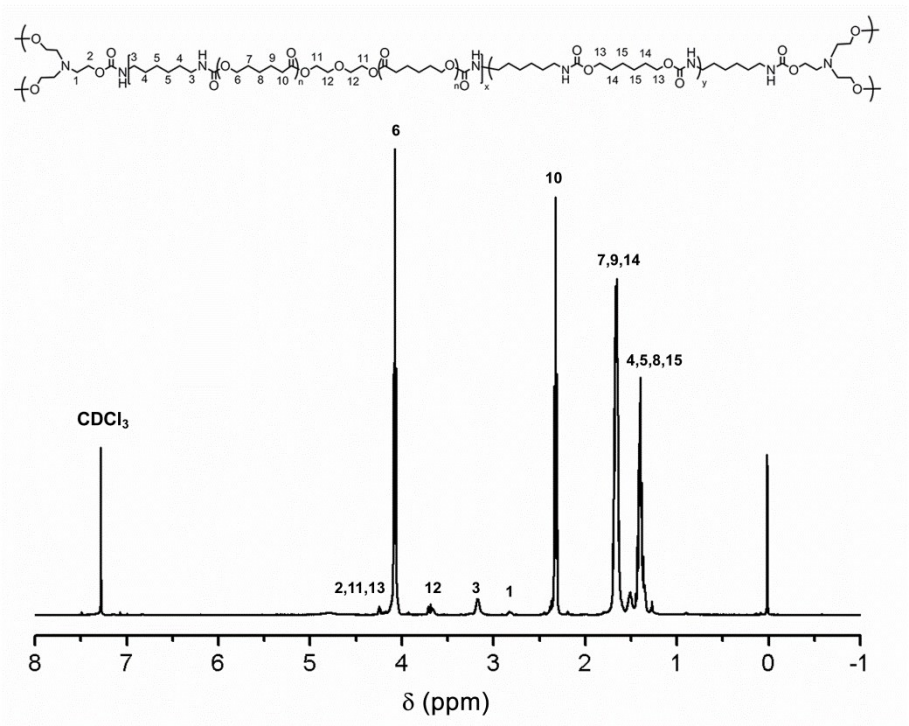

Fig. S1 ^{1}H NMR spectrum ($CDCl_3$) of PU network.

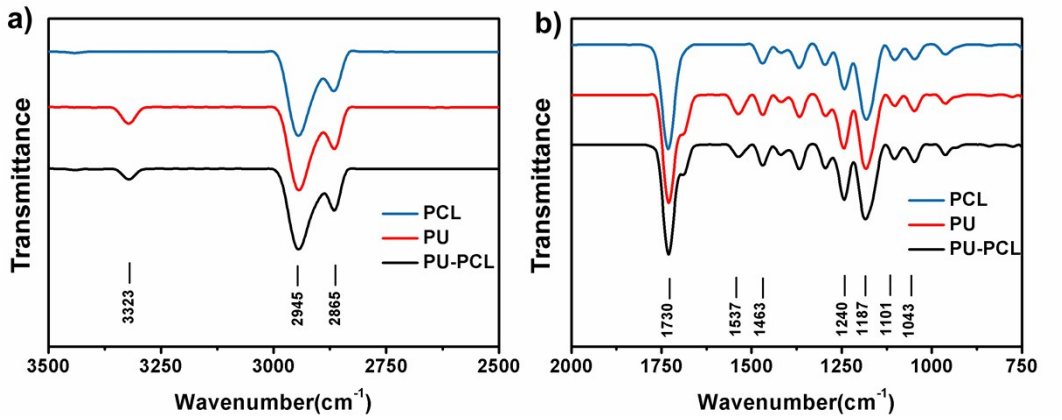

Fig. S2 FTIR spectra of liner PCL, PU and PU-PCL. The following characteristic peaks confirm the chemical structures: 3323 cm^{-1} (ν(-NH-)), 2945 and 2865 cm^{-1} (ν(CH_3, CH_2)), 1730 cm^{-1} (ν_{as}(C=O)), 1537 cm^{-1} (δ(C-N-H)), 1463 cm^{-1} (δ(CH_2)), 1240 and 1101 cm^{-1} (ν(C-O-C)), 1043 cm^{-1} (δ(C-O-C)), 1187 cm^{-1} (ν(OC-O)).

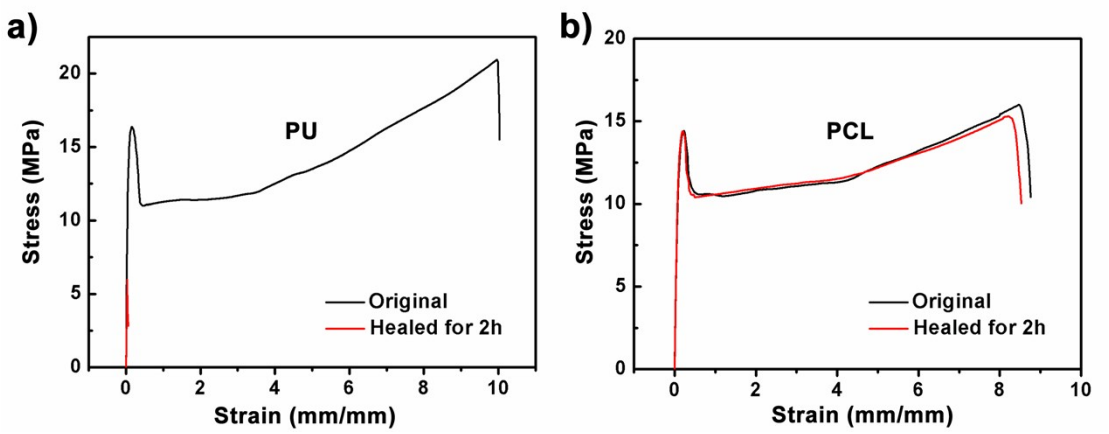

Fig. S3 (a) Stress-strain curves of the original and 2 h recontacted PU network samples that were previously cut into two pieces. (b) Stress-strain curves of the original and 2 h healed liner PCL samples that were previously cut into two pieces.

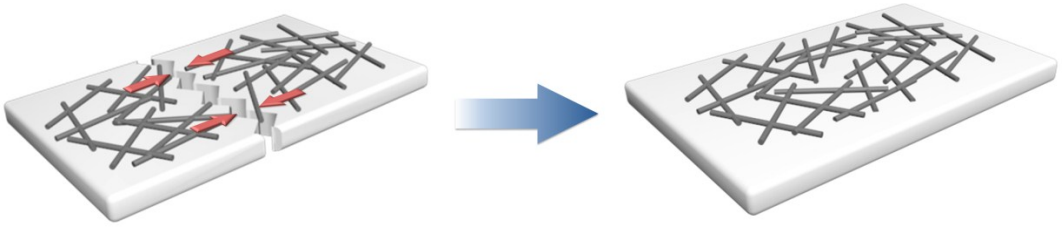

Fig. S4 Schematic illustration of healing process of CNTs/PU-PCL electrode.

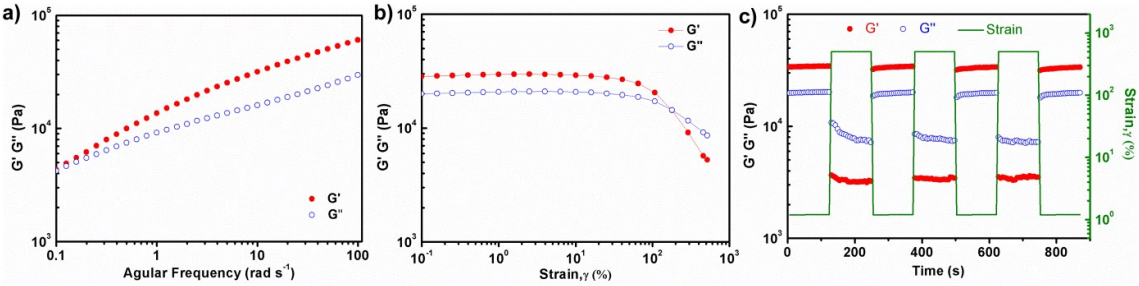

Fig. S5 Mechanical properties and self-healing behavior of PAA-PEO hydrogels. (a) Frequency-dependent (at a strain of 1%) oscillatory shear rheology of the hydrogel. (b) Strain sweep measurements of PAA-PEO hydrogel at 25 °C (storage modulus G′

and loss modulus G″ as a function of strain γ). (c) Repeated dynamic strain step tests (γ = 1% or 500%) of PAA-PEO hydrogel at 25 °C.

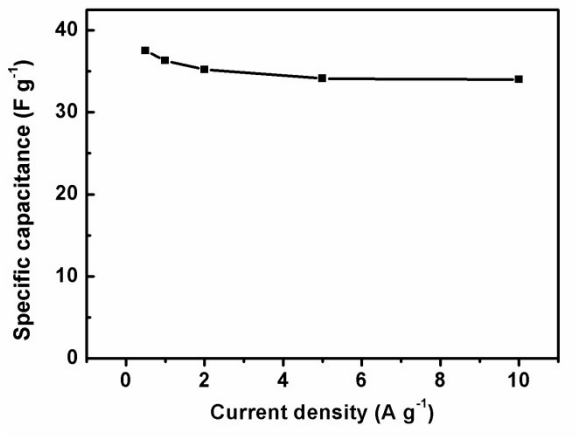

Fig. S6 Specific capacitance of the supercapacitor at different constant current densities.

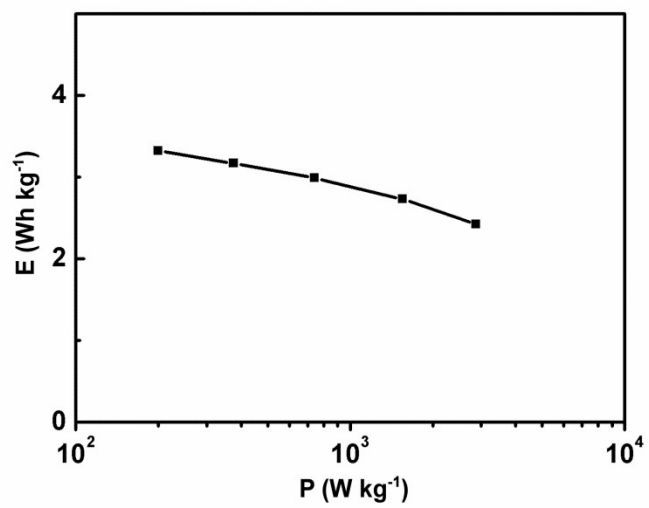

Fig. S7 The Ragone plot of supercapacitor.

The energy density (E, Wh kg^{-1}) and power density (P, W kg^{-1}) of the supercapacitor were calculated according to the following equations:

$E = [(C_{sp} \times \Delta V^2)/2] \times (1000/3600)$

$P = E/\Delta t$

where ΔV (V) is the actual voltage excluding IR drop of the discharge process, Δt (s) is the discharge time.

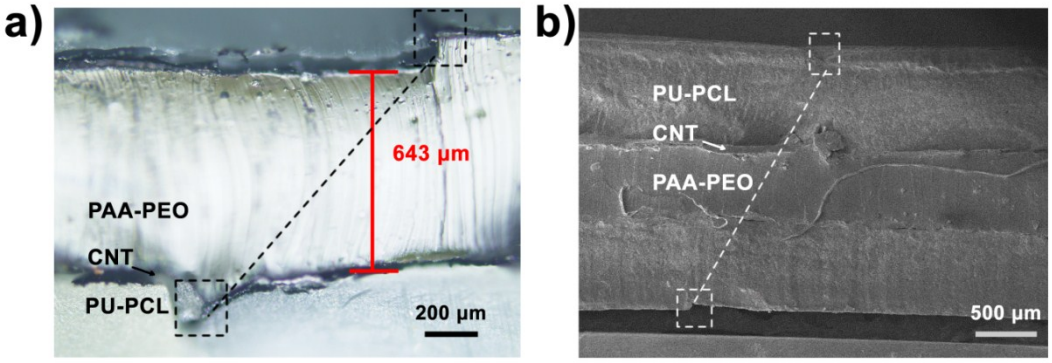

Fig. S8 (a) Optical microscopic image of the cross-section of the healed supercapacitor. (b) Cross-sectional SEM image of the healed supercapacitor. The dashed line indicates the cut in the original supercapacitor. The squares indicate the defects in the healed region of the supercapacitor

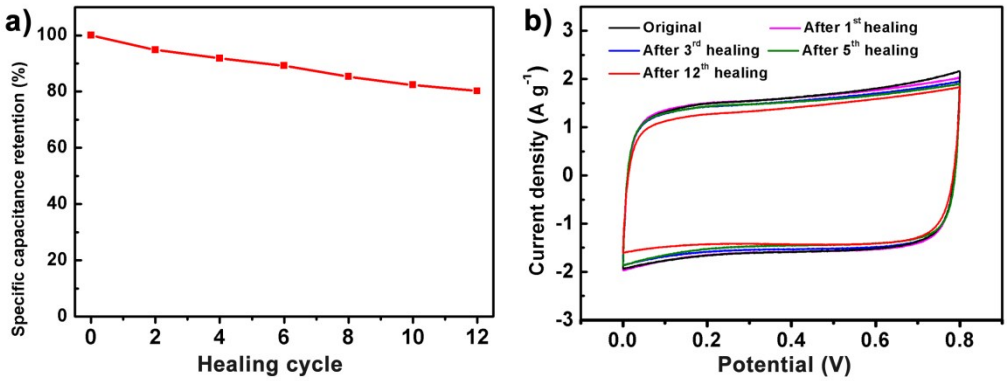

Fig. S9 Specific capacitance (a) and CV curves (b) of the original supercapacitor before and after different cutting/healing cycles.

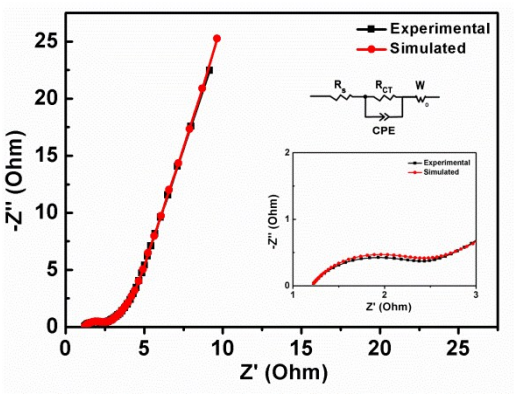

Fig. S10 Experimental and Simulated Nyquist plots of the original supercapacitor. Inset indicates the equivalent circuit used for simulating the experimental impedance data.

Table S1 The resistance values for the original supercapacitor and the same supercapacitor after different cutting/healing cycles.

Sample	R_s (Ω)	R_{ct} (Ω)
Original	1.16	1.74
After 1st healing	1.41	1.99
After 3rd healing	1.52	2.68
After 5th healing	1.64	3.16

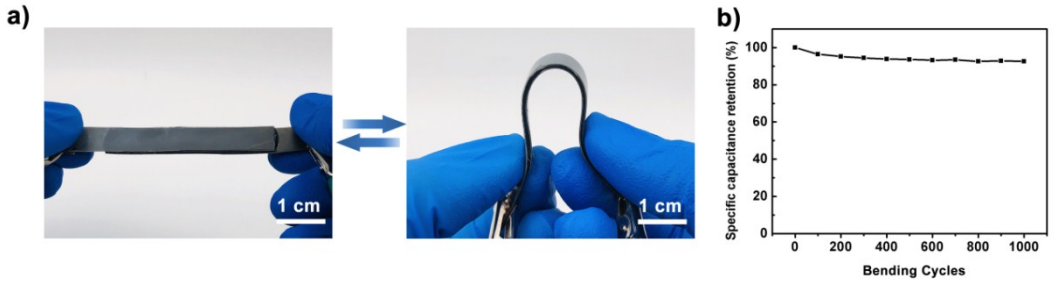

Fig. S11 (a) Optical images of the original supercapacitor and bent supercapacitor (~180°). (b) Specific capacitance retention of the supercapacitor as a function of repeated bending and recovery cycles.